ELSEVIER

Journal of Power Sources 54 (1995) 383–388

JOURNAL OF POWER SOURCES

Dependence of the morphology of graphitic electrodes on the electrochemical intercalation of lithium ions

D. Billaud [a], F.X. Henry [a], P. Willmann [b]

[a] *Laboratoire de Chimie Minérale Appliquée, Université de Nancy I, BP 239, 54506 Vandoeuvre-lès-Nancy Cedex, France*

[b] *Centre National d'Etudes Spatiales, 18 avenue Edouard Belin, 31055 Toulouse Cedex, France*

Abstract

We have studied the effects of several parameters that influence the electrochemical intercalation of lithium ions into various carbonaceous materials: massive samples of pyrographite PGCCL (Le Carbone Lorraine), bulky pitch-based graphitized carbon fibres P100-S (Amoco) and divided natural graphite powder UF4 (Le Carbone Lorraine). The electrochemical Li^+ intercalation has been achieved in electrolytic solutions composed of a solvent, ethylene carbonate and a conducting salt, $LiClO_4$. We have shown previously that such an electrolyte allows the intercalation of unsolvated lithium ions up to the richest stage-I LiC_6 composition without apparent solvent decomposition. The electrochemical behaviour of the electrodes in such electrolytes was followed either by chronopotentiometry (galvanostatic charge/discharge cycles) or by cyclic voltammetry. The use of microcomputers, able to conduct the experiments by imposition of charge or potential steps followed by cell relaxations, has allowed to obtain data on the kinetics of Li^+ intercalation. The electrochemical behaviour of the graphitic electrode is strongly dependent on its morphology. Moreover, the decrease of the size of the crystalline domains during prolongated cyclings has been shown particularly in massive pyrographite samples. Such an electrochemical grinding of the electrode has obviously a positive effect on its performances characterized by a noticeable increase in the maximum x composition reached (x refers to the Li_xC_6 composition). It appears also that the use of poly(vinylidene difluoride) (PVDF) leads to side reactions that have a negative effect on the performances of the electrodes.

Keywords: Electrodes; Graphite; Lithium ions; Intercalation

1. Introduction

Rechargeable lithium batteries offer high energy density. However, the most difficult technical problem to be overcome in their development is the poor cycling efficiency of the lithium electrode due to the dendritic growth of deposited lithium and to its reactions with the electrolyte or the impurities of the electrolyte.

The use of replacement materials such as lithium alloys and particularly the lithium–aluminium system, did not lead to significant improvements. In fact, large differences in the volume of these alloys appear during cycling which generates consequently mechanical stress and cracks leading to the destruction of the electrode [1–4].

To avoid these problems, the use of lithium ion intercalation anodes at low potentials appears as a promising solution [5]. Recent data have shown that some carbonaceous materials offering high cycleability may be suitable as lithium host electrode. Several parameters that influence the intercalation of lithium ions into carbons such as type of carbon, nature of the binders and electrolyte compositions have been studied [6–10]. The effect of CO_2 and organic materials as additives was also studied [10].

It is known for several years that lithium in gaseous, liquid or solid state can react with graphite to form lithium–graphite intercalation compounds characterized by their stage number defined as the number of carbon sheets separating two successive intercalated layers [11–13]. These direct reactions of lithium with graphite allow the obtention of the LiC_6 stage-I compound. Previous attempts to obtain LiC_6 by electroreduction of graphite in liquid electrolytes were unsuccessful [14,15]. Moreover, in certain electrolytes, co-insertion of solvent molecules or reduction of the inserted solvent leads to graphite exfoliation [16].

In contrast with these previous works, our recent investigations have shown that unsolvated Li^+ ion could be electro-intercalated into pyrographites in liquid electrolytes such as $LiClO_4$/ethylene carbonate (EC) and that the rich LiC_6 composition could be obtained [17–20].

SSDI 0378-7753(94)02107-E

A new electrolyte of unknown composition and reported by Tarascon et al. [21] allows also the use of graphite as a negative electrode in which the LiC_6 composition is obtained.

Our former studies were carried out on massive samples such as pieces of pyrographite since the oriented structure of this type of material is very suitable to perform X-ray diffraction (XRD) characterization. In fact, we have identified and characterized the different intercalation stages which appear during the electrochemical intercalation and de-intercalation processes [17,20]. The effects of the current density on the kinetics of the Li^+ intercalation/de-intercalation reactions have appeared to be enhanced in massive samples. For example, lithium plating on the surface of the graphite electrode can occur concomitantly with the formation of LiC_6 if the current density is too high. In this paper, we will compare the electro-intercalation of lithium ions into different graphitic materials: massive pyrographite, pitch-based graphitized fibres and divided natural graphite.

2. Experimental

Oriented pyrolytic graphite PGCCL (Le Carbone Lorraine) was used after being cut and cleaved in parallelepipeds suitable for in situ XRD studies. Pitch-based graphitized carbon fibres P 100-S (Amoco) were used after being heated at 700 °C for 12 h under secondary vacuum in order to remove their protective films. Divided natural graphite UF4 (Le Carbone Lorraine) of particle size smaller than 20 μm was also treated in the same way as the P 100-S fibres. Lithium perchlorate, $LiClO_4$, was dried at 180 °C under secondary vacuum before utilization. Ethylene carbonate (EC) (Aldrich) was outgassed under dynamic secondary vacuum. Intercalation was performed either in a three-electrode cell or in a two-electrode device: lithium foils were used as reference and counter electrodes; the working electrode is either a piece of pyrographite or a set of fibres cut into pieces of about 15 mm in length and attached vertically at one end between two metallic plates acting as a current collector. The other end of the fibres was soaked in the electrolyte, avoiding contact between the metallic collector and the electrolyte. Experiments with divided graphite were carried out using a plastified electrode (7–8 wt.% poly(vinylidene difluoride) (PVDF). The electrolyte used was a solution of $LiClO_4$ in EC (1–1.5 mol $LiClO_4$/kg EC).

XRD studies were carried out using either a $\theta/2\theta$ goniometer operating with the Mo Kα radiation or a curvated detector associated with a rotating molybdenum anticathode and performed directly through the electrolysis cell in order to avoid contamination or degradation of the samples studied. The electrochemical experiments were conducted with a PAR 273 potentiostat/galvanostat working either in galvanostatic or voltammetry mode. A Mac Pile potentiostat/galvanostat was also used to obtain curves in the neighbourhood of the thermodynamical equilibrium [22].

3. Results and discussion

3.1. Pyrographite

Fig. 1 shows two potential–composition $E(x)$ curves (x refers to the formula Li_xC_6) recorded during the second and third galvanostatic charge of a PGCCL electrode ($m=4.94$ mg) in $LiClO_4$/EC (1 M/kg EC) electrolyte at 51 °C and at two different current intensities, 10 and 25 μA, respectively. These curves present potential slopes corresponding to the stoichiometry domain of a pure phase and plateaus related to the transformation of a stage s to a stage $(s+1)$ [17]. XRD studies performed during the intercalation wave allowed the identification of the different stages s based on their identity period along c-axis, I_c, and their interplanar spacing, d_I, according to the relationship:

$$I_c\ (\text{Å}) = d_I + (s-1)3.35 \quad (1)$$

These two curves are superimposed to the formation potential of the LiC_{12} stage-II compound. Beyond this value, the potential decreases to 0 V where lithium deposition occurs. It appears that this zero potential is obtained for x close to 0.82 in the case of the second charge at $I=10$ μA, and for x close to 0.62 for a third charge at $I=25$ μA. The influence of the current density on the kinetics of the intercalation reactions is therefore clearly demonstrated. The $Li_{0.82}C_6$ and $Li_{0.62}C_6$ compositions correspond in reality to a mixture of pure LiC_{12} stage-II and LiC_6 stage-I. Pure stage-I can be obtained after application of the electrolysis current but, in these conditions, LiC_6 formation and lithium deposition occur simultaneously.

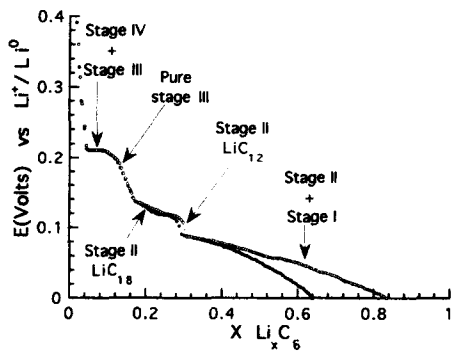

Fig. 1. Second and third galvanostatic charges of a PGCCL sample performed at electrolysis current densities of (○) 2.02 μA/mg and (●) 5.06 μA/mg, respectively.

Fig. 2 presents, for comparison, the previous charge curve (cycle No. 3) and the tenth charge obtained with the same PGCCL sample in identical experimental conditions: electrolysis current equals to 25 μA, for the same electrolyte composition. It appears that the x value reached at zero potential increases when the cycle number is also increased. For cycle No. 3, x is found equal to 0.62 while for cycle No. 10, x is equal to 0.86. Such an increase in the electrochemical capacity with the cycle number is related to transformations in the morphology of the pyrographite sample; we found that repetitive redox cycles are related to an important decrease in the crystalline domain size of the graphitic host structure. The domain size is characterized by the coherence length values L_c and L_a along graphite c- and a-axis, respectively, obtained by XRD studies from measurements of the full width at half-maximum of the (004) and the (110) Bragg peaks. In these conditions, the access of lithium ions to the internal part of the electrode is facilitated [23].

Cyclic voltammetry experiments have been performed with the Mac Pile system on PGCCL samples, as presented in Fig. 3. The mass of graphite is equal to 9.43 mg and the electrolyte is composed of EC and $LiClO_4$ (1.34 M/kg EC). The potential allowed to vary by steps of 1.25 mV for 0.625 h. Then, the cell is relaxed up to the moment that the electrolysis current is lower than 1 μA. The temperature of the cell is kept at 50 °C. Three peaks can be observed during the reduction (intercalation) process. They correspond, respectively, to stage-IV/stage-III, stage-III/stage-II and stage II/stage-I transformations. Two main peaks appear in the oxidation wave (de-intercalation): the broader one is related to the concomitant transformation of both stage-I and stage-II into a stage-III; the last peak represents the stage-IV formation. It appears consequently that the kinetics of intercalation is different from that of de-intercalation since in the de-intercalation process, in our experimental conditions, lithium extraction from stage-I and stage-II occurs simultaneously.

The importance of the kinetic aspects is particularly demonstrated in Fig. 4 which presents two discharge curves of LiC_6 carried out at two different values of the electrolysis current. The curve achieved at 32.1 μA is shifted towards potential values higher than those obtained at the 8 μA intensity. Moreover, the potential plateau appearing in Fig. 4(a) around 0.23 V and corresponding to the stage III/stage IV transformation is not anymore visible in Fig. 4(b).

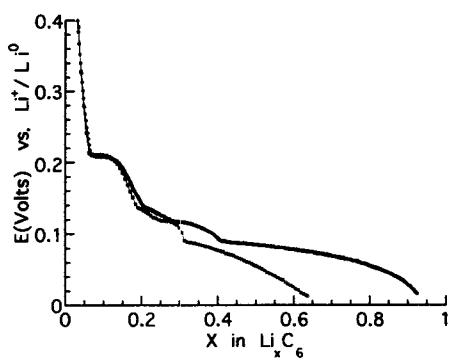

Fig. 2. Third and tenth galvanostatic charges of the PGCCL sample of Fig. 1 obtained for the same electrolysis current of 25 μA: (O) third cycle, and (●) tenth cycle.

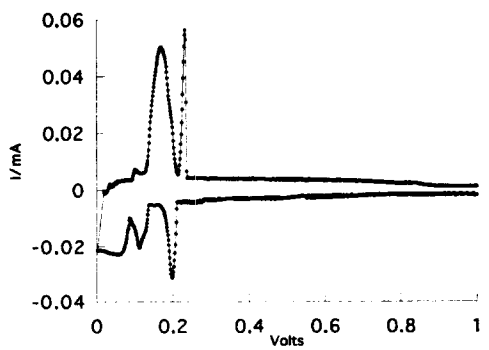

Fig. 3. Cyclic voltammogram performed on a PGCCL sample (9.43 mg) in $LiClO_4$/EC (1.34 M/kg EC) electrolyte at 50 °C.

3.2. Pitch-based carbon fibres

Pitch-based carbon fibres treated at high temperatures (2600–2800 °C) to achieve their graphitization appear as attractive candidates for lithium intercalation. Their textures in cross section are strongly dependent on the experimental conditions of elaboration [24]. Among these pitch-based fibres, those presenting open textures

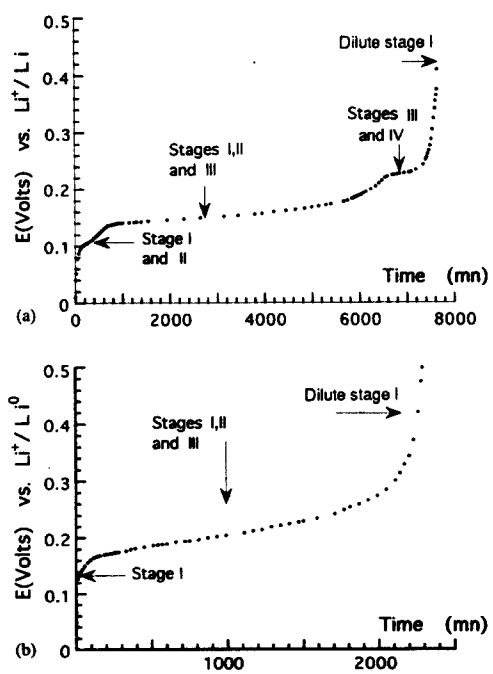

Fig. 4. First constant current discharge of the system Li/$LiClO_4$–EC/PGCCL at (a) 8 μA and (b) 32.1 μA.

are the most suitable for their utilization as anode of secondary batteries. In this study, we have selected the P100-S fibres (Amoco). The cross-section scanning electron microscopy (SEM) micrograph of such a fibre is given in Fig. 5. Before use, these fibres were heat-treated to remove additional products. They have been characterized by XRD studies in order to obtain the characteristics of their crystalline domains. We found that the coherence lengths, L_c and L_a, are equal to 130 and 98 Å, respectively [23]. Fig. 6(a) shows the fifth and the sixth charge/discharge cycles carried out on massive P100 fibres at 9.96 and 14.88 μA/mg, respectively, in $LiClO_4$/EC (1.5 M/kg EC). Both cycles are perfectly superimposed which shows that the influence of the current density on the kinetics of intercalation is less important with materials exhibiting large specific areas. Even lower current densities of 1.88 μA/mg does not modify the shape of the related charge curve also given in Fig. 6(a). The special morphology of the P100 fibres allows consequently the intercalation or de-intercalation of Li^+ to occur with a faster kinetics than that is observed in massive samples such as pyrographites. It must be pointed out that, despite this faster kinetics, only the apparent $Li_{0.72}C_6$ composition was obtained in these fibres. As a matter of fact, the rich LiC_6 composition was reached. The difference observed in these compositions could be due to the presence of amorphous, non-graphitized parts of the fibres or to the existence of graphitized domains inaccessible for Li^+ penetration, at least for the first charge/discharge cycle. For prolongated cycling, the electrochemical 'grinding' of the above-described carbon material for massive PGCCL samples, in which the decrease in the crystalline domain size was correlated with the increase in cycle number, could also occur in the fibres. Therefore, the maximum capacity x should be drawn near 1. Studies on the evolution of the fibre morphology during prolongated cyclings are now in progress [23].

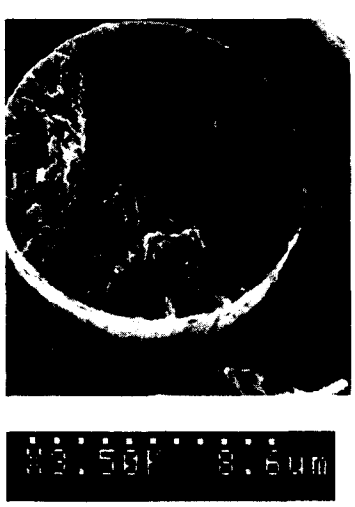

Fig. 5. Morphology of a graphitized P100 fibre observed by scanning electron microscopy.

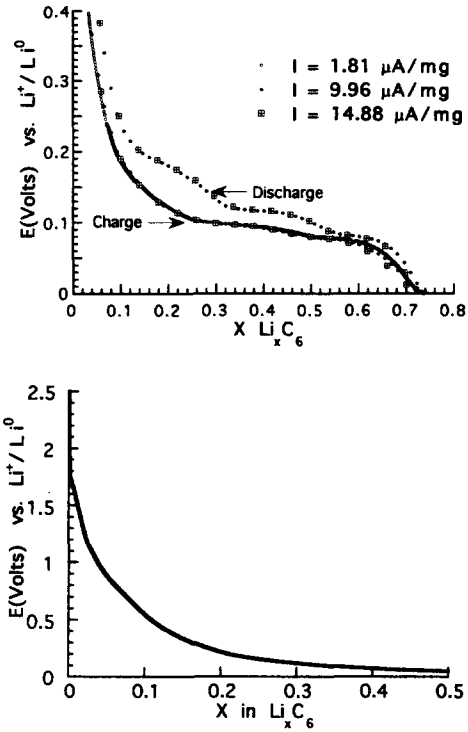

Fig. 6. (a) Charge and discharge curves of massive P100 fibres recorded at 1.81, 9.96 and 14.88 μA/mg. (b) The charge curve obtained after integration of a part of a first voltammogram performed on the same massive P100 fibres.

Fig. 6(b) shows a curve obtained after integration of the first cyclic voltammogram performed on the massive P100 fibres in the same $LiClO_4$/EC electrolyte as described for the experiments presented in Fig. 6(a). The potential values decrease regularly from the initial 2.5 V value.

3.3. Divided UF4 graphite

Finally, intercalation of lithium has been carried out in divided UF4 graphite (Le Carbone Lorraine). The particle size of this type of graphite is in the range from 0 to 20 μm as shown in the SEM micrograph presented in Fig. 7. This graphite is outgassed under secondary vacuum. A composite electrode with UF4 as the active material (92 wt.%) and PVDF as a binder (8 wt.%) is formed at the surface of a titanium plate working as electron collector.

Fig. 8(a) gives the first charge/discharge cycle of a composite electrode UF4 (92.5 wt.%)–PVDF (7.5 wt.%) in galvanostatic mode. The mass of the active material (UF4) is equal to 12.16 mg. The electrolysis current of -120 μA is applied for 0.2 h. After each current application, the cell is allowed to rest for 0.025 h. The initial potential close to 3.5 V decreases sharply to 1.7 V. Then a shoulder is observed at around 1 V. After that, the decrease in potential is roughly similar to that observed with PGCCL or P100 fibre samples. It must,

Fig. 7. Morphology of divided UF4 graphite observed by scanning electron microscopy.

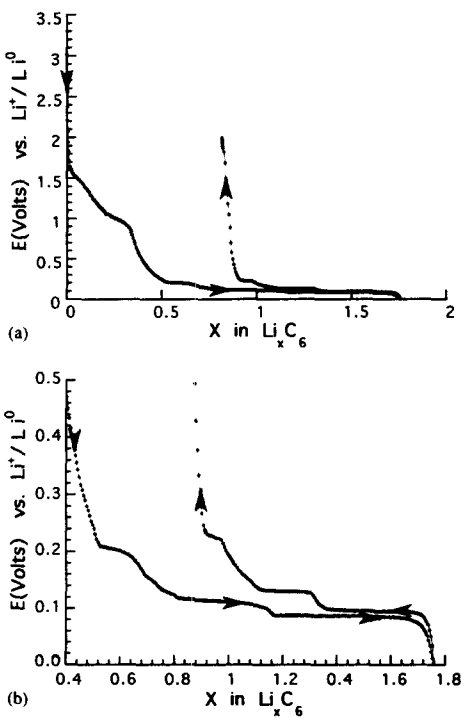

Fig. 8. First charge/discharge cycle in galvanostatic mode of a composite electrode composed of graphite UF4 (92.5 wt.%) and PVDF (7.5 wt.%): (a) electrolysis current equal to -120 μA between 3.5 and 0 V, and (b) between 0.5 and 0 V (enlarged scale).

however, be noticed that the maximum x value reached at 0 V is equal to 1.75. It appears that, in our experimental conditions, simultaneous reactions occur during the charge process. The binder, PVDF, obviously is chemically not inert. The shoulder at around 1 V has been previously attributed to the formation of a passivating layer formed during the reduction of the electrolyte on the electrode surface [8,25]. The reduction of impurities or groups linked at the surface of the composite electrode have also to be taken into account. Work is now in progress to study the effects of such side reactions. The discharge curve presented in Fig. 8(a) presents well-defined potential slopes separated by horizontal plateaus. The slope corresponding to stage-I/stage-II transformation is perfectly apparent. Such characteristics can be better observed in Fig. 8(b) which is part of Fig. 8(a), with an extended scale between 0.5 and 0 V. The potential values corresponding to the stage transformations are thus very well defined. Fig. 9(a) and (b) shows the second charge/discharge cycle obtained with the same electrode as that of Fig. 8. The maximum x value at 0 V is slightly higher than 1. This can be due either to the formation of a compound a slightly richer in metal than LiC_6 or to the signature of some of the side reactions mentioned ahead. The shoulder at around 1 V observed during the first charge has disappeared. Here also, stage-I/stage-II transformation is clearly observed in the discharge curve around the expected theoretical composition $Li_{0.5}C_6$ corresponding to the metal-rich stage-II compound. The Δx value measured between 2.3 and 0 V is equal to 1.

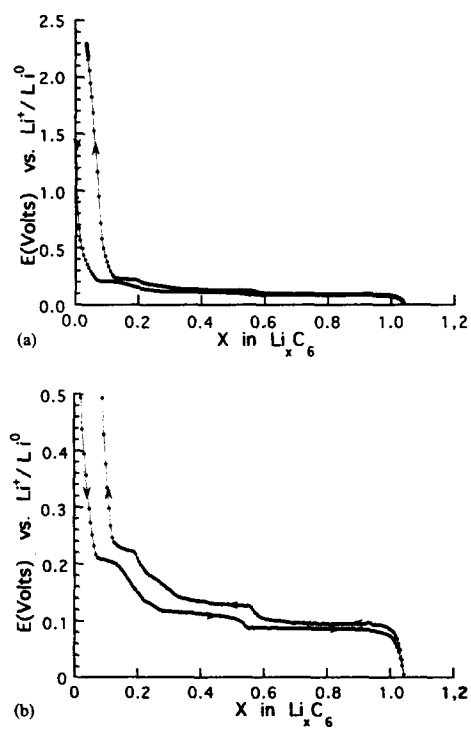

Fig. 9. (a) Second charge/discharge cycle obtained with the same electrode as described in Fig. 8. (b) Enlarged scale of (a) between 0.5 and 0 V.

4. Conclusions

Some aspects related to the influence of the morphology of the carbonaceous materials on the kinetics of Li^+ intercalation and on the maximum values of the electrochemical capacity have been shown. In bulky materials such as PGCCL pieces, the influence of the current density is very important since lithium plating on the graphite electrode can occur well before the total completion of LiC_6 formation. Thus, if the current density is too high, lithium plating and LiC_6 formation occur simultaneously. However, prolongated charge/discharge cycles result in a decrease of the crystalline domain size with a concomitant increase of the maximum x value reached. Such an electrochemical grinding effect tends to counter-balance the influence of the current density. Bulky pitch-based graphitized fibres such as P100 fibres are much less influenced by the current density. The maximum x value obtained with these fibres ($x=0.72$) is far enough from the theoretical $x=1$ value. This could be due to the special texture of the fibres in which the possibility to find some graphitized parts inaccessible to lithium ions has to be taken into account. A grinding of these fibres in small-sized particles could lead to a partial opening of the closed domains. Such studies are now in progress.

Finally, our experiments on graphite powders such as UF4 graphite set a problem related to the use of the binder. The too high maximum x values obtained at 0 V and during the first charge seem to be related to side reactions involving the binder PVDF, at least in our experimental conditions with the $LiClO_4$/EC electrolyte. The existence of a shoulder around 1 V, usually attributed in the literature to the formation of a passivating layer, is only visible with the graphite powder. There is no evidence for such an important shoulder with P100 fibres although the active surface in these materials is high. Work on divided fibres is in progress to study the possible relationship between the active area and the formation of this passivating layer.

Acknowledgements

The work at the University of Nancy was supported in part by a C.N.E.S. grant.

References

[1] K.M. Abraham, J.S. Foos and J.L. Goldman, *J. Electrochem. Soc., 131* (1984) 2197.
[2] R.A. Huggins, *J. Power Sources, 26* (1989) 109.
[3] J.O. Besenhard, *J. Electroanal. Chem., 94* (1978) 77.
[4] T. Landoldt-Börnstein, *Structure Data of Elements and Intermetallic Phases*, Vol. 6, Springer, Berlin, 1971.
[5] M. Armand, in D.W. Murphy, J. Broadland, B.C.H. Steeles (eds.), *Materials for Advanced Batteries*, Plenum, New York, 1980.
[6] R. Kanno, Y. Takeda, T. Ichikawa, K. Nakanishi and O. Yamamoto, *J. Power Sources, 26* (1989) 535.
[7] M. Mohri, N. Yanagisawa, Y. Tajima, H. Tanaka, T. Mitate, S. Nakajima, M. Yoshida, Y. Yoshimoto, T. Suzuki and H. Wada, *J. Power Sources, 26* (1989) 545.
[8] R. Fong, U. von Sacken and J.R. Dahn, *J. Electrochem. Soc., 137* (1990) 2009.
[9] P. Schoderböck and H.P. Boehm, *Mater. Sci. Forum, 91* (1992) 6424.
[10] O. Chusid, Y.E. Ely, D. Aurbach, M. Babai and Y. Carmeli, *J. Power Sources, 43/44* (1993) 47.
[11] D. Guérard and A. Hérold, *C.R. Acad. Sci. Paris, 275 C* (1972) 571.
[12] D. Billaud and A. Hérold, *Carbon, 17* (1979) 183.
[13] D. Billaud, E. McRae and A. Hérold, *Mater. Res. Bull., 14* (1979) 857.
[14] J.O. Besenhard, *Carbon, 14* (1976) 111.
[15] M. Arakawa and J. Yamaki, *J. Electroanal. Chem., 219* (1987) 273.
[16] P. Willmann, *Thesis*, University of Nancy, 1979.
[17] D. Billaud, F.X. Henry and P. Willmann, *Mater. Res. Bull., 28* (1993) 477.
[18] D. Billaud, F.X. Henry and P. Willmann, *Proc. 18th Int. Power Source Symp., Stratford-on-Avon, 19–21 Apr. 1993.*
[19] P. Willmann, D. Billaud and F.X. Henry, *Proc. European Space Power Conf., Graz, Austria, 23–27 Aug. 1993*, p. 789.
[20] D. Billaud, F.X. Henry and P. Willmann, *Mol. Cryst. Liq. Cryst., 245* (1994) 159.
[21] J.M. Tarascon, D. Guyomard and G.L. Baker, *J. Power Sources, 43/44* (1993) 689.
[22] C. Mouget and Y. Chabre, in *Multichannel Potentiostat Galvanostat 'Mac Pile'*, licensed from CNRS and UJF Grenoble to Biol-Logic Co., Claix, France.
[23] F.X. Henry, D. Billaud and P. Willmann, to be published.
[24] N. Imanishi, H. Kashiwagi, T. Ichikawa, Y. Takeda and O. Yamamoto, *J. Electrochem. Soc., 140* (1993) 315.
[25] B. Simon, J.P. Boeuve and M. Broussely, *J. Power Sources, 43/44* (1993) 65.